

**UNCLASSIFIED**

**AD 404 889**

**DEFENSE DOCUMENTATION CENTER**

**FOR**

**SCIENTIFIC AND TECHNICAL INFORMATION**

**CAMERON STATION, ALEXANDRIA, VIRGINIA**



**UNCLASSIFIED**

NOTICE: When government or other drawings, specifications or other data are used for any purpose other than in connection with a definitely related government procurement operation, the U. S. Government thereby incurs no responsibility, nor any obligation whatsoever; and the fact that the Government may have formulated, furnished, or in any way supplied the said drawings, specifications, or other data is not to be regarded by implication or otherwise as in any manner licensing the holder or any other person or corporation, or conveying any rights or permission to manufacture, use or sell any patented invention that may in any way be related thereto.

63-3-5

404889

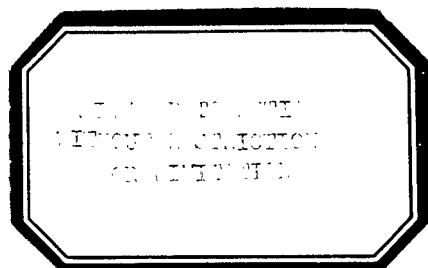
# **ELECTROMAGNETIC COUPLING TO ORDNANCE SYSTEMS**

Prepared For

**THE U. S. NAVAL WEAPONS LABORATORY  
DAHLGREN, VA.**

404 889

**Final Report  
Contract N178-7921  
December 31, 1962**



# **ELECTROMAGNETIC COUPLING TO ORDNANCE SYSTEMS**

**Prepared For  
THE U. S. NAVAL WEAPONS LABORATORY  
DAHLGREN, VA.**

**Final Report  
Contract N178-7921  
December 31, 1962**

## ABSTRACT

This report presents a procedure for analyzing the transmission of energy from electromagnetic radiators to electrically initiated devices of ordnance systems. Techniques of measurement and problem areas are discussed.

A method is presented for examining the spatial perturbations of an electromagnetic field aboard ship. The deviations of the field strength from an unperturbed, free-space field are examined as a statistical function.

## ELECTROMAGNETIC COUPLING TO ORDNANCE SYSTEMS

### 1.1 Introduction

This work is concerned with the hazards of electromagnetic radiation to ordnance (HERO). The object of the work is to develop theoretical and experimental techniques for the analysis of coupling between sources of electromagnetic energy and electrically initiated ordnance devices. A theoretical approach to analysis of the HERO problem was developed and reported under an earlier Naval Weapons Laboratory Contract. Sufficient material from this report is contained here for continuity.

Three specific tasks in support of the general objectives of the contract have been completed. These are a handbook of electro-explosive devices, <sup>2</sup> supplements to an index of electromagnetic radiating devices, <sup>3</sup> and a survey of the HERO status of Naval weapons. <sup>4</sup>

### 2.1 Analysis of Electromagnetic Coupling

Three areas of HERO analysis are considered in this report. These are (a) transmission analysis, (b) transmission measurement techniques, and (c) the probability distribution of shipboard electromagnetic fields.

Electromagnetic energy from shipboard radio equipment reaches the electroexplosive device (squib) within an ordnance element by a complex transmission route involving several modes of coupling and various degrees of attenuation. Usually only a small fraction of the source energy reaches the squib. The degree of safety, or hazard, is determined by the extent to which this undesired energy approaches or exceeds the energy required to initiate the squib.

In shipboard HERO tests, it is usually considered sufficient to measure only the energy (or some related quantity, such as power, voltage, current or bridge wire temperature rise) actually reaching

---

1. Reference 1
2. Reference 2
3. Reference 3
4. Reference 4

the squib. Whereas these tests are sufficient to determine the degree of safety or hazard of the weapon under the conditions of the test, many vital questions are not answered by this procedure. Some of these unanswered questions are: (a) What would be the effect of moving the weapon to another shipboard location? (b) What hazard would result from adding another transmitting antenna? (c) Could a hazard occur due to some error in connecting the weapon to its launcher? (d) How could the probability of a hazard be reduced?

To answer these and other questions it is necessary to analyze the transmission path between the electromagnetic source and the squib, to measure some of the transmission parameters, and to measure or compute the distribution of electromagnetic field strengths aboard the ship. Many of the measurements, computations and analyses require time and laboratory facilities that best can be made available at shore installations such as Naval weapons laboratories and ordnance test stations.

This work is intended to illustrate some of the procedures which can be used to analyze the HERO problem.

## 2.2 Transmission Analysis

The energy required to initiate a squib is only a minute fraction of the energy delivered to various electromagnetic radiators in the vicinity of shipboard ordnance. Reliability of the ordnance and safety of personnel depend upon adequate isolation of the squib from the potentially hazardous electromagnetic energy.

One measure of the attenuation between the squib and energy source is given as the ratio of the source power to the power actually delivered to the squib. For example, if 1000 watts delivered to a nearby transmitting antenna produces 1 watt in an ordnance device squib, the attenuation between squib and transmitter is 1000:1, or 30 decibels.

Part of this attenuation is obtained by physical separation of the ordnance device from the transmitting antenna. Aboard ship, however, space attenuation is frequently negligible. Missile launchers, aircraft, and other ordnance apparatus can act as very efficient receiving antennas. It is not unusual for the radio frequency (RF) energy available from an aircraft fuselage, acting as a receiver of

environmental RF energy, to far exceed that required to initiate a squib.

Additional attenuation is obtained by shielding the squib and its firing circuit, isolating the firing circuit from the shield and other current-carrying members of the weapon, and, if necessary, by filters. The ability to determine not only the total attenuation but also the attenuation provided by each of these factors is essential to the understanding of many HERO problems. An example will illustrate the transmission analysis procedure.

Figure 1 shows a missile being hoisted into position for electrical connection to the underside fuselage of an aircraft located on a ship's deck adjacent to a radio transmitting antenna. A radio transmitter (not shown) produces antenna voltage and current,  $V_1$  and  $I_1$ . The aircraft fuselage, missile, and hoist, acting as a receiving antenna, develops a voltage  $V_s$  between the unconnected ends of the firing circuit shield (terminals 2-2'). When these ends are connected, current  $I_s$  flows between the aircraft and the missile along the firing circuit shield.

Now, assume that the aircraft end of the firing circuit shield accidentally comes in contact with the missile firing circuit so that current  $I_s$ , instead of flowing along the missile skin, actually flows into the missile, as shown in Figure 2.

Figure 2 shows the squib (terminals 3-3') at one end of a transmission circuit being supplied with RF energy from the aircraft and missile skin which now are acting as a receiving antenna.

Figure 3 shows the complete transmission system between the radio transmitting antenna input terminals 1-1' and the squib, terminals 3-3'.

The object of this example is to illustrate the procedure for determining the attenuation of each part of the transmission system and the total system attenuation.

In transmission analysis it is convenient to define three quantities in the following manner, using the four terminal network between terminal pair 1-1' and 2-2' of Figure 2 for an example:

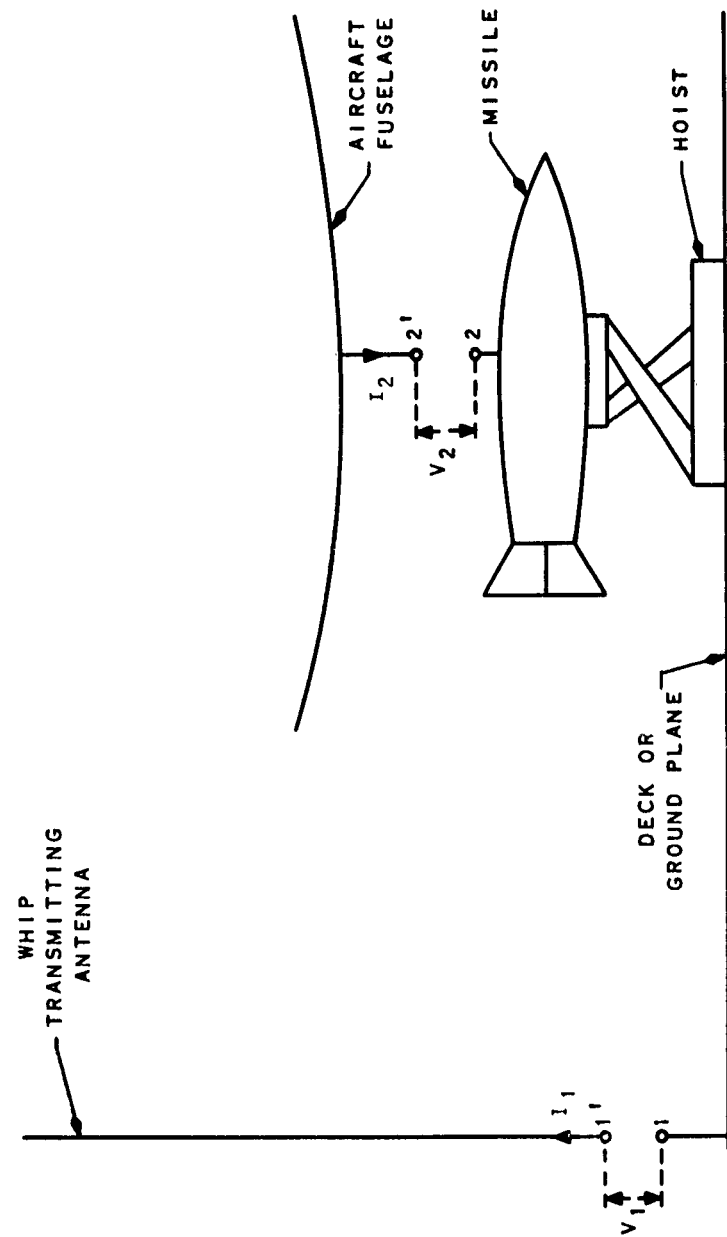


Figure 1. A Missile in the Process of Being Electrically Connected to an Aircraft.

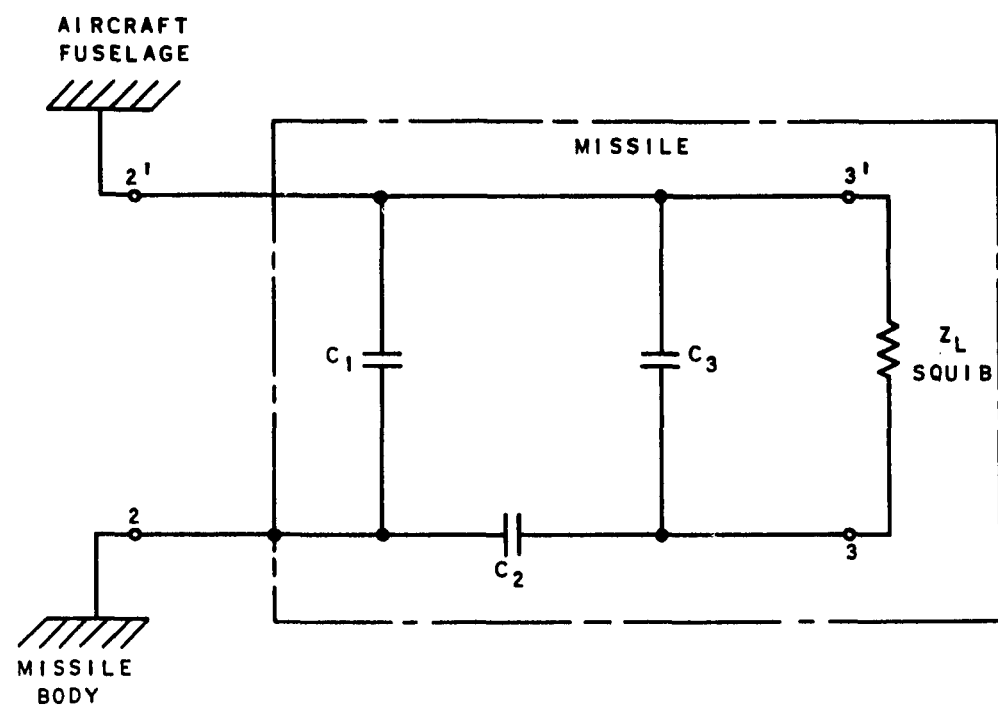


Figure 2. The Schematic Circuit of the  
Missile During Connection.

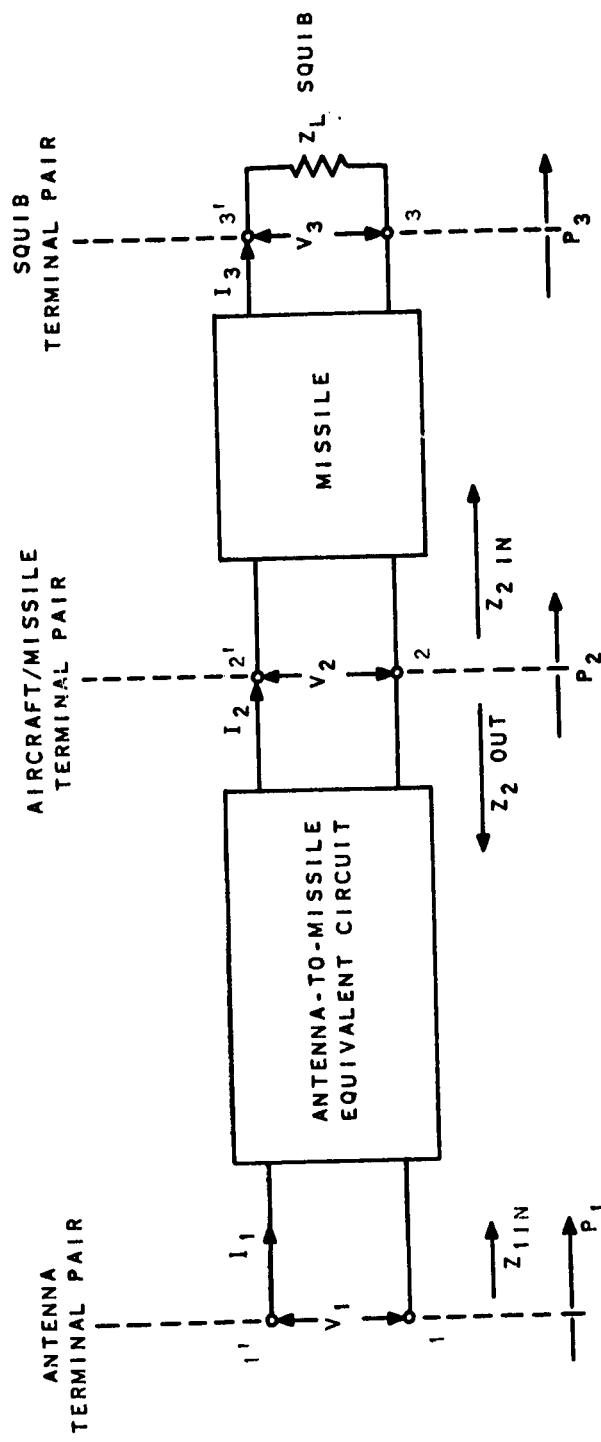


Figure 3. Nomenclature and Equivalent Circuits Between Antenna and Squib Terminals.

$$A_{1-s} = \frac{P_s}{P_i} \quad (1)$$

where  $A_{1-s}$  is the attenuation of a four terminal network having input power  $P_i$  and output power  $P_s$ .

$$K_{I(1-s)} = \frac{P_s \text{ max}}{P_i} \quad (2)$$

where  $K_{I(1-s)}$  is the insertion loss of the four terminal network having maximum available output power,  $P_s \text{ max}$ , (i.e., into a conjugate impedance load) when the input power is  $P_i$ .

$$K_{R2} = \frac{P_s}{P_s \text{ max}} \quad (3)$$

where  $K_{R2}$  is the reflection factor of a four terminal network capable of delivering maximum available power output,  $P_s \text{ max}$ , (into a conjugate impedance load) but actually delivering  $P_s$  output power into a mismatched load.

Thus, the attenuation,  $A_{1-s}$ , is the product of the insertion loss and the reflection factor

$$A_{1-s} = K_{I(1-s)} \cdot K_{R2} \quad (4)$$

Taking the logarithms of Equation 4, the attenuation, insertion loss and reflection loss in decibels are

$$10 \text{ Log } A_{1-s} = 10 \text{ Log } K_{I(1-s)} + 10 \text{ Log } K_{R2} \quad (5a)$$

Substituting lower case letters to represent the corresponding logarithmic terms, Equation 4 becomes

$$a_{1-s} = k_{I(1-s)} + k_{R2} \quad (5b)$$

Correspondingly, the total attenuation  $a_{1-s}$  between the antenna input, terminals 1-1', and the squib, terminals 3-3', becomes

$$a_{1-s} = k_{I(1-s)} + k_{R2} + k_{I(s-s)} + k_{R3} \quad (6)$$

Thus, the total attenuation of any number of tandem-connected four terminal networks is the sum of insertion losses of the individual

networks plus the sum of the reflection factors for each interface.<sup>5</sup>

The transmission system shown in Figure 3 has two networks and the squib connected in tandem. It should be observed, however, that the second network (i.e., the missile) is composed of lossless components only (see Figure 2). Thus,  $P_3 = P_2$ . Consequently, it is necessary only to compute the attenuation  $a_{1-2}$  between the transmitting antenna input, terminals 1-1', and the missile input, terminals 2-2', as in Equation 5.

The insertion loss of the network between the transmitting antenna input and the missile input,  $k_{I(1-2)}$ , can be computed from measured values using Equations 7 and 8.

$$K_{I(1-2)} = \frac{1}{4R_1 \text{ in } R_2 \text{ out}} \left| \frac{E_{a \text{ oc}}}{I_1} \right|^2 \quad (7)$$

$$k_{I(1-2)} = 10 \text{ Log } K_{I(1-2)} \quad (8)$$

where  $E_{a \text{ oc}}$  is the voltage between terminals 2-2' when these terminals are open-circuited.

Next, an expression for the reflection factor,  $K_{R2}$ , at the interface terminals 2-2' is derived. Recalling the definition of the reflection factor, Equation 3,

$$K_{R2} = \frac{P_2}{P_{2 \text{ max}}}$$

and its logarithmic expression in decibels,

$$k_{R2} = 10 \text{ Log } K_{R2} \quad (9)$$

---

5. Generally, a reflection factor term is included for the interface between the transmitter and the input terminals. This term is omitted here because the transmitter power output is held constant (returned, etc.) to compensate for loading or detuning which might otherwise be caused by proximity of the aircraft.
6. Another form of Equation 7 was given in Reference 1, p. 22, Equation 2 - 6, with slightly different nomenclature. Here, the subscript "in" means measurements looking toward the load, and "out" refers to measurements made looking toward the generator.

the expressions for  $P_s$  and  $P_{s \text{ max}}$  are found to be<sup>7</sup>

$$P_s = E_s \text{ oc} \frac{R_s \text{ in}}{|Z_s \text{ in} + Z_s \text{ out}|^s} \quad (10)$$

and

$$P_{s \text{ max}} = \frac{E_s \text{ oc}}{4R_s \text{ out}} \quad (11)$$

where  $E_s \text{ oc}$  is the voltage measured between terminals 2-2' with these terminals open-circuited (i.e., with the missile disconnected).

The ratio of  $P_s$  to  $P_{s \text{ max}}$  is

$$K_{R2} = \frac{P_s}{P_{s \text{ max}}} = \frac{4R_s \text{ in} \cdot R_s \text{ out}}{|Z_s \text{ in} + Z_s \text{ out}|^s} \quad (12)$$

Having obtained expressions for the total attenuation between antenna input terminals and the missile input terminals in terms of the insertion loss and reflection factors, it is now possible to examine the total attenuation in terms of its constituent parts.

The values of voltage, current, and impedances ( $E_i$ ,  $I_{asc}$ ,  $Z_{i \text{ in}}$  and  $Z_{s \text{ out}}$ ) as functions of frequency were obtained from an actual aircraft and transmitting antenna measurements.\*

The missile input impedance,  $Z_{s \text{ in}}$ , is

$$Z_{s \text{ in}} = 0.25 - j \frac{400}{f_{mc}} \quad (13)$$

where  $f_{mc}$  is the frequency in megacycles per second.

Figure 4 shows the relative power levels (in decibels) between the transmitting antenna input and missile input. The transmitter power output is used as the reference (zero db) level. The maximum no-fire squib power ( $P_0$  expressed in decibels) is shown as 30 db below the reference transmitter power output. (This corresponds

---

7. The significance of the subscripts "in" and "out" are given in footnote 6.  
 8. See Reference 1, pp 22-26.

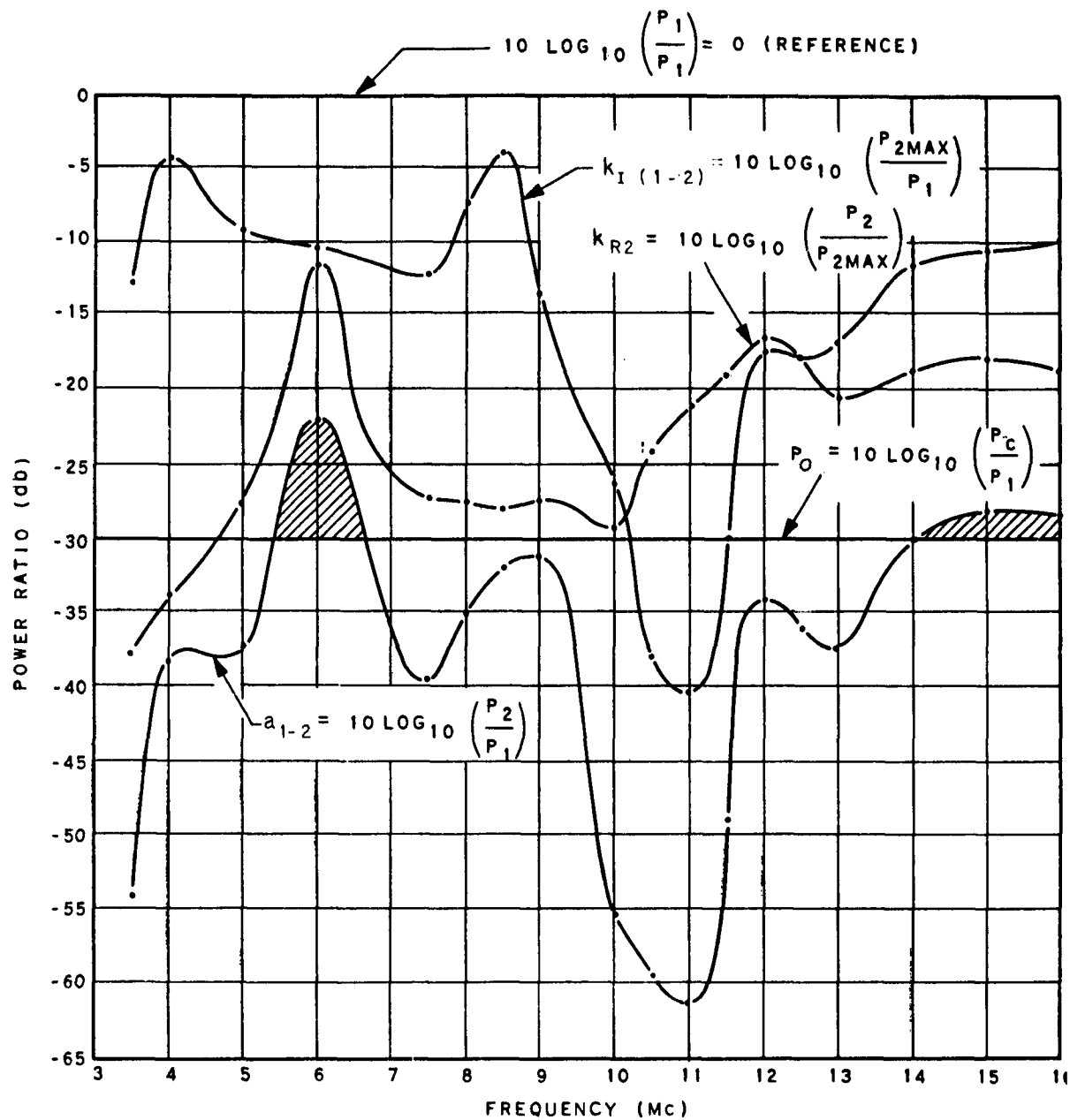


Figure 4. Relative Power Levels in the Antenna-Missile System.

to a 1 watt no-fire squib and a 1000 watt transmitter output, for example.)

Curves are also given in Figure 4 for insertion loss  $k_{I(1-s)}$  between antenna and missile input, for the reflection factor,  $k_{R2}$ , due to impedance mismatch at the junction between aircraft and missile, and for the total attenuation,  $a_{1-s} = a_{1-3}$ ; that is,  $a_{1-s}$  is also the total attenuation between transmitting antenna input and the squib.

The two cross-hatched areas between the total attenuation curve  $a_{1-s}$  and the maximum no-fire squib power level,  $P_0$ , indicate the extent to which the power delivered to the squib exceeds the maximum no-fire power level.

Many other useful observations can be made by referring to Figure 4. The curve of  $k_{I(1-s)}$  indicates that very little attenuation was obtained by the spatial separation between aircraft and transmitting antenna—less than 5 db near 4 Mc and 8.5 Mc, and less than the required 30 db over the entire frequency range except between 10.25 Mc and 11.5 Mc.\*

The reflection factor curve  $k_{R2}$  (Figure 4) indicates a large mismatch between the aircraft and the missile input impedance below 4.5 Mc (greater than 30 db) and a resonance at 6 Mc with only 12 db attenuation.

The value of the approach to transmission analysis given here is the ease with which the various coupling parameters may be separately evaluated. Part of this advantage derives from the use of energy (or power) relationships rather than voltage or current ratios. The second advantage comes from expressing power ratios in terms of the maximum available power.

The use of power rather than voltage or current is consistent with the fact that both the squib maximum no-fire power and the trans-

---

9. The large value of insertion loss,  $k_{I(1-s)}$ , at 11 Mc indicates that the transmitting antenna and the "receiving antenna" consisting of the aircraft, missile and hoist were, at that frequency, substantially decoupled from each other. The significance of this observation is not apparent; however, it suggests the possibility of "decoupling" ordnance devices from adjacent transmitting antennas.

mitter output power are constant over significant ranges of frequency.

Expressing power ratios in terms of maximum available power gives a direct appraisal of limiting conditions of power transfer. Unfortunately, however, the more sensitive electrical measurement instruments (below the microwave range) are voltmeters rather than watt meters. Further consideration of transmission measurements is given below.

### 2.3 Transmission Measurement Techniques

Before considering measurement techniques and instruments, a review of the electrical parameters which must be measured is appropriate.

The transmission analysis presented earlier requires information on the following electrical parameters: The impedance looking each direction at each subsystem interface and some factor which defines the electromagnetic coupling between the transmitting antenna and the ordnance system used as a "receiving antenna". In antenna practice, this coupling factor is called the mutual impedance and is the ratio of the open circuit voltage produced in one antenna to the current in the second antenna. Thus, the last factor in the expression for the insertion loss (Equation 7) is the mutual impedance. It should be pointed out, however, that the insertion loss is a power ratio; the choice of electrical parameters required to express input power and maximum available output power is a matter of convenience. For example, it may be more convenient to read a watt meter to obtain  $P_1$  when operating a ship's transmitter, and to read a voltmeter or ammeter and an impedance bridge when operating with test instruments.

Unfortunately, the choice of electrical measurement instruments is not so flexible when working at the very low power levels and when making measurements without some convenient "ground" surface.

Space limitations make it necessary to locate impedance bridges and voltmeters at significant distances from the terminals of the circuit to be measured. The cable or leads used to connect the instrument to the circuit must be arranged in such a way that extraneous factors are avoided or sufficiently minimized. This is not always possible to accomplish with an instrument of appreciable physical size, especially if either of the terminals of the instrument is coupled to the instrument case.

Some of the problems of measurements and suggested solutions can be illustrated by an example. Suppose that it is desired to measure the voltage of the circuit between terminals 3-3' of Figure 2. Two problems appear immediately. First, there is no space inside the missile for the voltmeter. Second, neither of the terminals (3-3') is at "ground" potential. Within the skin of the missile, at least, "ground" might be considered to be the missile skin. Then, a voltmeter having one side "grounded" to the missile skin might be used to measure the voltage from missile skin to each of the terminals 3-3'. The voltage between terminals 3-3' is the difference of these two voltages, provided, of course, that the phase difference of the voltages is also taken into account. Here a third difficulty is encountered; that is, the requirement for a phase-indicating voltmeter. A fourth problem is the requirement for correcting the indicated voltage for circuit voltage changes caused by the voltmeter input and cable impedances. Fortunately, the analysis procedure of Section 2.2 requires voltage current or power measurements at only one point in the transmission system other than at the input to the transmitting antenna. Analysis of the voltmeter problem will continue, however, because the ability to measure voltages on the transmission circuit is an asset and, further, some of the voltmeter problems also are encountered with impedance bridges.

The solutions to some of the voltmeter problems can be discussed by reference to Figure 5. Here, it is seen that the voltmeter has been located outside the missile and connected to the missile with a section of coaxial cable having a characteristic impedance,  $Z_0$ , equal to the voltmeter input impedance  $Z_m$ . The shield of the voltmeter cable is connected to the missile skin (terminal 2). The inner conductor of the voltmeter cable may be connected either to terminal 3 or terminal 3'. Thus, it is the intention to measure the voltages between terminals 2-3 and terminals 2-3' and to compute, if possible, the voltage between terminals 3-3'.

Expressing the voltmeter readings in terms of the unperturbed voltages, the circuit impedances, and the input impedance of the voltmeter cable, the expression for the voltage across terminals 3-3' is obtained.

$$V_{3-3'} = V'_{1-s} \left( 1 + \frac{Z_{1-s}}{Z_m} \right) - V'_{1-s'} \left( 1 + \frac{Z_{1-s'}}{Z_m} \right) \quad (14)$$

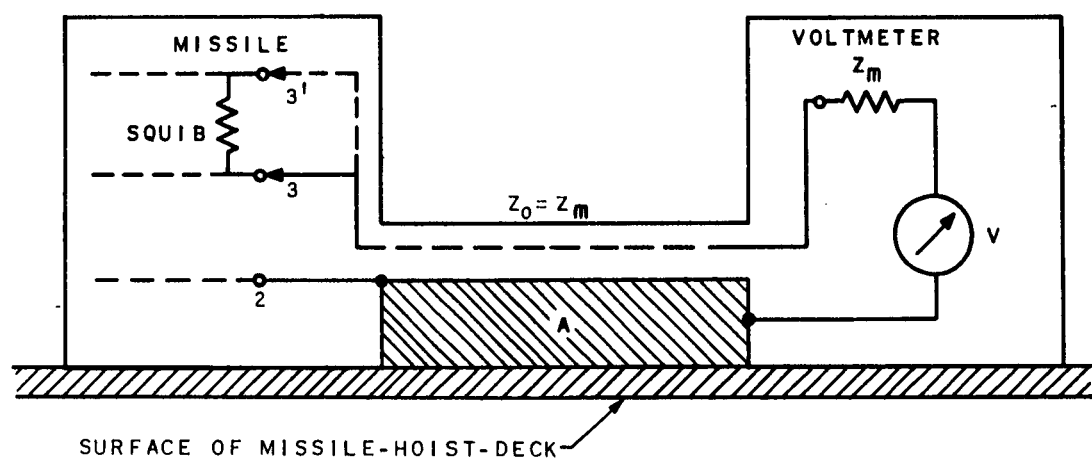


Figure 5. Arrangement for Measuring Squib Voltage.

where  $V'_{1-s}$  and  $V'_{1-s'}$  are the voltmeter readings; the transmission circuit impedances to the missile skin are  $Z_{1-s}$  and  $Z_{1-s'}$ .

The bracketed terms are the correction factors to be applied to the voltmeter readings. These factors approach unity as the voltmeter cable input impedance approaches infinity, giving,

$$V'_{3-s} = V'_{1-s} - V'_{1-s'} \quad (15a)$$

when

$$Z_m \gg Z_{1-s} \text{ and } Z_{1-s'} \quad (15b)$$

Recall that the voltages in Equations 15 are vector quantities. Then, the voltmeter readings are nearly useless unless phase information can be obtained. A fortunate situation occasionally arises in which one of the voltmeter readings is much greater than another. If the two readings differ by 10 times, or more, the total voltage can be taken to be the greater of the two readings with an angle error of less than 6 degrees and a magnitude error of 10 percent or less.

The precautions which must be observed in order to locate the voltmeter outside the missile skin are to prevent extraneous coupling to the transmission circuit and to prevent undesired energy from reaching the voltmeter. These problems are greatly reduced by locating the voltmeter on a relatively large equipotential surface, such as the deck or ground plane (see Figures 1 and 5), and by dressing the voltmeter cable as close as possible to a relatively large, low impedance structure, such as the missile skin and hoist. The object is to reduce the area between the cable and the adjacent structure (the shaded area, A, in Figure 5). Some current will flow, nevertheless, along the voltmeter cable. The cable shield must join the missile (and voltmeter) skins through a continuous low impedance connection, completely surrounding the cable, and having a minimum of electric or magnetic coupling to the interior regions.

The difficulty of voltage measurements in ordnance work has stimulated investigations of other measurement techniques. One of the most successful approaches has been to measure some nonelectrical quantity associated with the energy delivered to the squib's bridge wire. This quantity might be temperature rise of the bridge wire, thermal

radiation, and other phenomena. A number of these techniques are listed below. For information on the various works, the references should be consulted.

Thermocouple<sup>10 11</sup> and thermistor<sup>12</sup> temperature detectors are being investigated by Denver Research Institute. Another organization, Measurement Systems, Inc., has investigated a so-called quantum detector<sup>13</sup> for measurement of thermal radiation from the bridge wire of a simulated squib. A novel method for measuring the heat energy of a bridge wire has been investigated by the Department of Physics of Randolph-Macon College.<sup>14</sup> Other methods which have been investigated by Denver Research Institute<sup>15</sup> include measurement of electron emission from the bridge wire and the use of pyroelectric materials.

Each of the above methods has the distinct advantage of relatively small perturbation of the measured quantity. The methods are limited to measurement at the output (squib) of the transmission system only and, thus, do not completely fill the needs for transmission measurement instruments.

One element of transmission analysis and measurement has been left, purposefully, to the last. This is the electromagnetic environmental field. The distribution of electromagnetic fields aboard ship is considered in the following section.

#### 2.4 Distribution of Electromagnetic Fields Aboard Ship

In Section 2.2, the analysis began at the input to the transmission system; i.e., with the power, voltage, or current input to the transmitting antenna. The next step was to determine the mutual impedance between the transmitting and "receiving" antennas. It is frequently desirable to consider the coupling in two steps. First, the electromagnetic field is related to the antenna input power, voltage, or current; second, the coupling between the electromagnetic field and the ordnance system, acting as a receiving antenna, is determined.

---

- 10. Reference 5
- 11. Reference 6
- 12. Reference 7
- 13. Reference 8
- 14. Reference 9
- 15. Reference 6

The second approach, that of considering the electromagnetic field as the "input" to the transmission system, is most convenient when several transmitting antennas are involved. Then, the spatial distribution of fields aboard the ship gives a very useful picture of an important aspect of the HERO problem; that is, the electromagnetic environment.

Field distributions aboard ship can be obtained either by measurements or by computation. Perhaps a great deal more confidence could be placed in measured data than in computations. However, in the case of a fairly wide-open deck, somewhat characteristic of the flight deck of an aircraft carrier, a reasonable degree of success could be expected from computations.

In this Section, a number of comparisons are made between measured and computed field distributions aboard an aircraft carrier. The work would be more-or-less academic if the object were only to compare computed and measured results. Actually, the object is to present the results of a large number of measurements made over very large areas of the ship in a manner that gives the probability distribution of the measured field about the unperturbed field. In other words, the measured field strength at each point has been normalized with reference to the half-plane free-space fields computed for the same points. The procedures are discussed in connection with three examples below.

Figure 6 shows one of the three areas of the USS Constellation (CVA-64) in which measurements were made<sup>16</sup> of the electric component of the field produced by the cage antenna No. 2-4 located above the ship's island. An A4D-2 aircraft, located at the center of the circle, was headed successively toward each of the twelve points (0100 through 1200). The electric field strength was measured at each point for each aircraft heading giving 144 readings. An additional twelve readings were made with the aircraft removed, for a total of 156 measured values.

---

16. The measurements were conducted jointly by the U.S. Navy, Bureau of Ships, and the U.S. Naval Weapons Laboratory. Details of the measurements and tabulation of data are given in Reference 10.

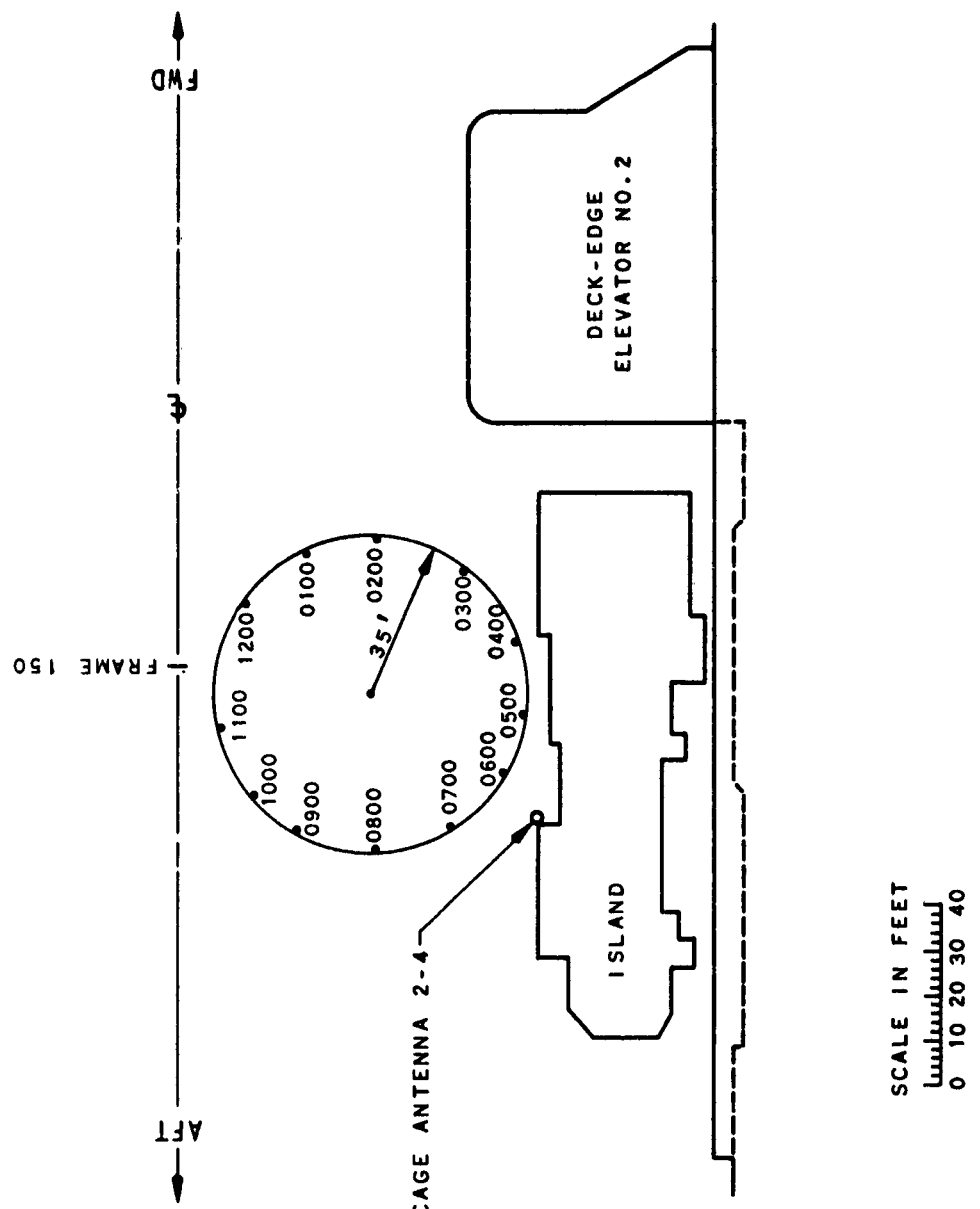


Figure 6. Plan View Showing Test Points for Field Strength Measurements at 9.215 Mc from Cage Antenna 2-4.  
 A4D-2 Aircraft Located at Center of Circle.  
 USS Constellation (CVA-64).

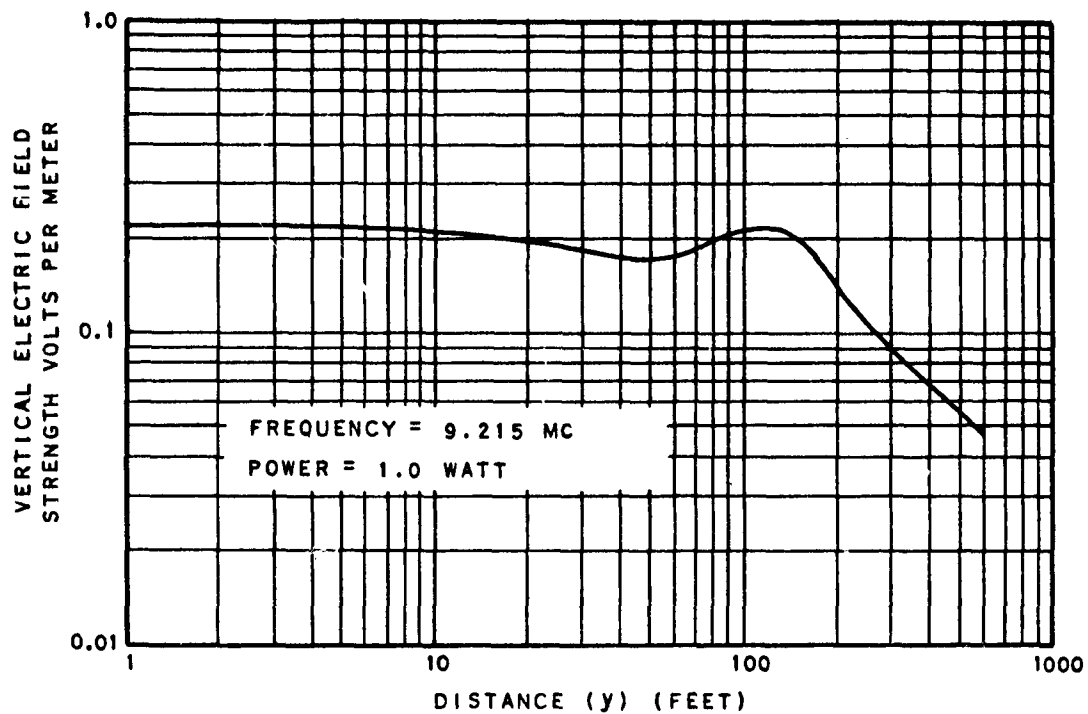
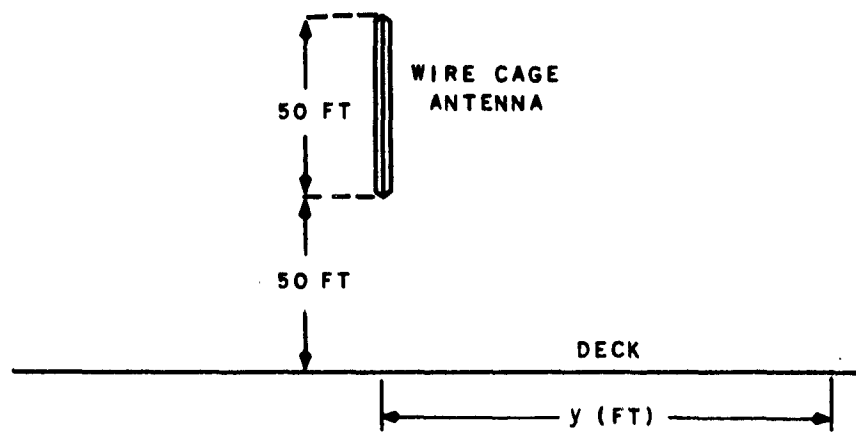


Figure 7. Electric Field Strength Produced by an Elevated, Vertical Antenna.

Figure 7 shows the somewhat idealized antenna length and height above deck.<sup>17</sup> For purposes of computation, the presence of the flight deck is ignored. Figure 7 also shows the computed vertical electric field strength versus distance measured along the deck. It is interesting to note that the computed free-space field varies only  $\pm 10$  percent over the entire area of the ship under consideration (from 12 feet to 82 feet).

Figure 8 shows the probability distribution of the ratio of computed and measured fields. A number of interesting and useful observations can be drawn from Figure 8. Since the computed field is essentially constant, it is apparent that the measured field varies over quite a wide range. The mean ratio of computed-to-measured fields is 0.72.

The logarithms of the ratios appear to have a nearly normal distribution. Suppose we define the ratio of computed-to-measured fields in terms of the logarithm of the ratio, as follows:

$$X = 20 \log \frac{E_c}{E_m} \quad (16)$$

and define the mean value of  $\bar{X}$  of  $N$  individual values of  $X_i$

$$\bar{X} = \frac{1}{N} \sum X_i \quad (17)$$

Then, the standard deviation,  $\sigma$ , of the  $X_i$  values about the mean  $\bar{X}$  is

$$\sigma = \frac{1}{N} \left| \sum (X_i - \bar{X})^2 \right|^{\frac{1}{2}} \quad (18)$$

Thus, the mean value,  $\bar{X}$ , of the field ratios expressed in decibels, is  $\bar{X} = 2.86$  decibels.

From Figure 8 it is found that the 95 percent and 5 percent probability limits correspond to field strength ratios of 0.36 and 3.5 respectively, or a 19.8 decibel variation in  $X_i$ . The  $X_i$  are

---

17. The antenna (No. 2-4) actually runs at an angle less than vertical and extends out slightly over the flight deck. The orientation is idealized for simplicity of computation.

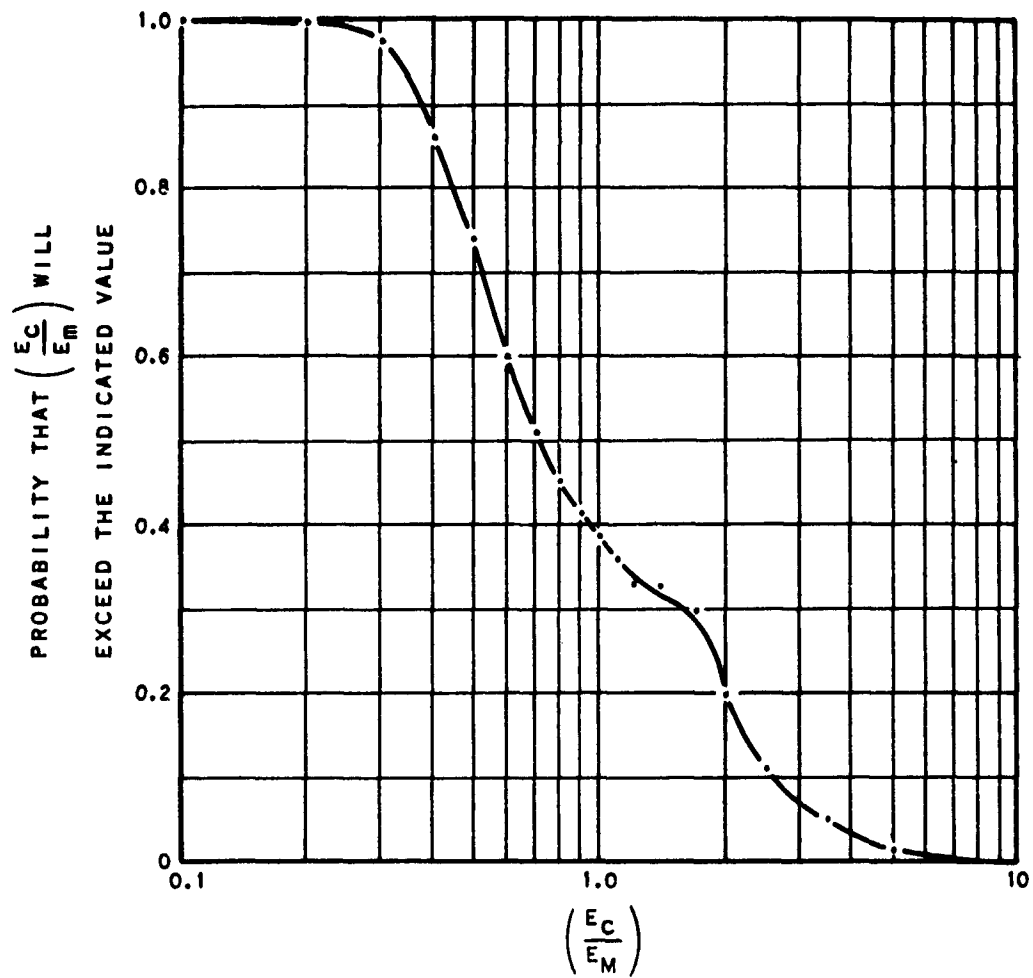


Figure 8. Probability Distribution of  $(E_c/E_m)$  for the Shipboard Area of Figure 6.

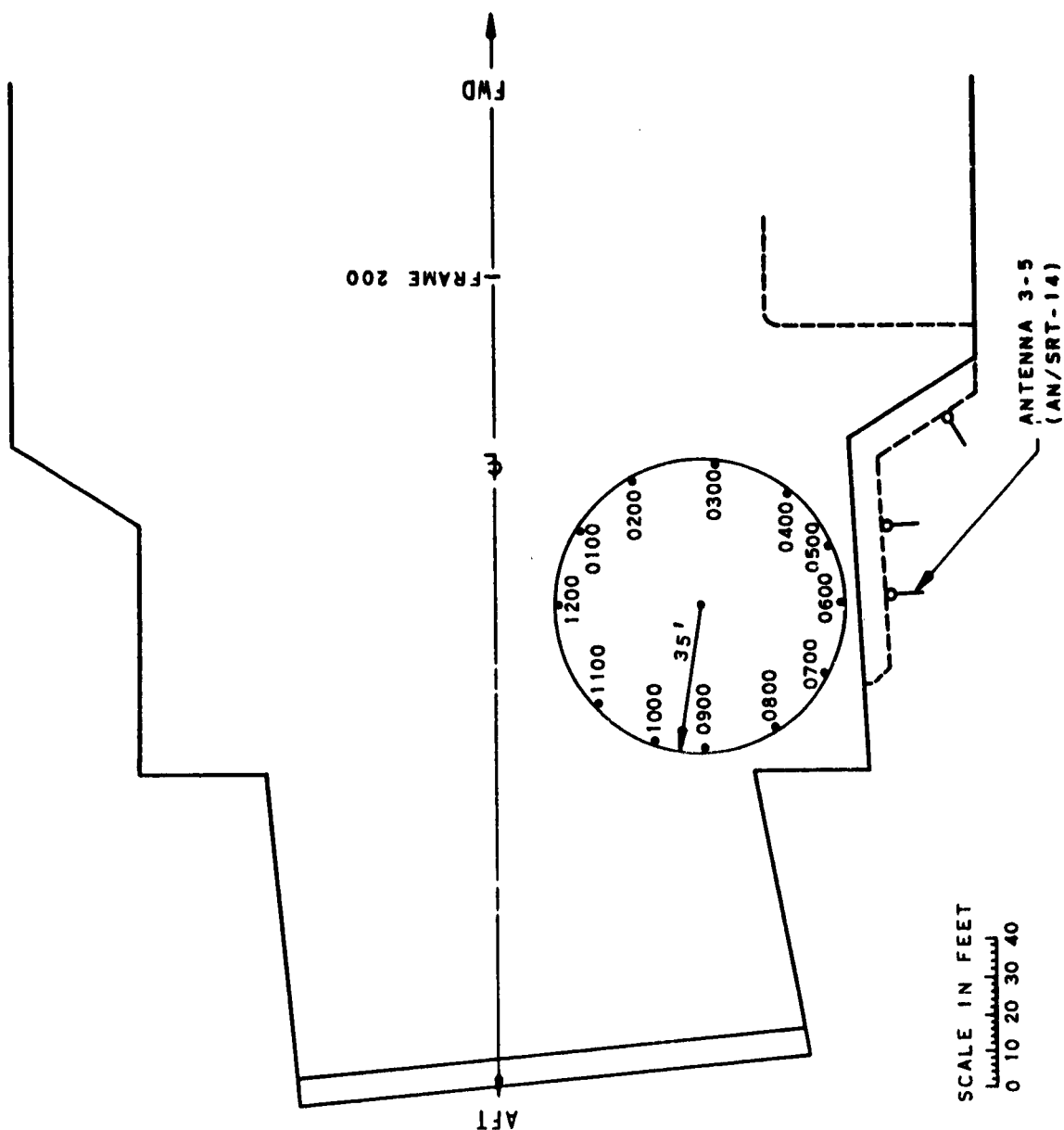


Figure 9. Plan View Showing Test Points for Field Strength Measurements at 9.215 Mc from Antenna 3-5.  
A4D-2 Aircraft Located at Center of Circle.

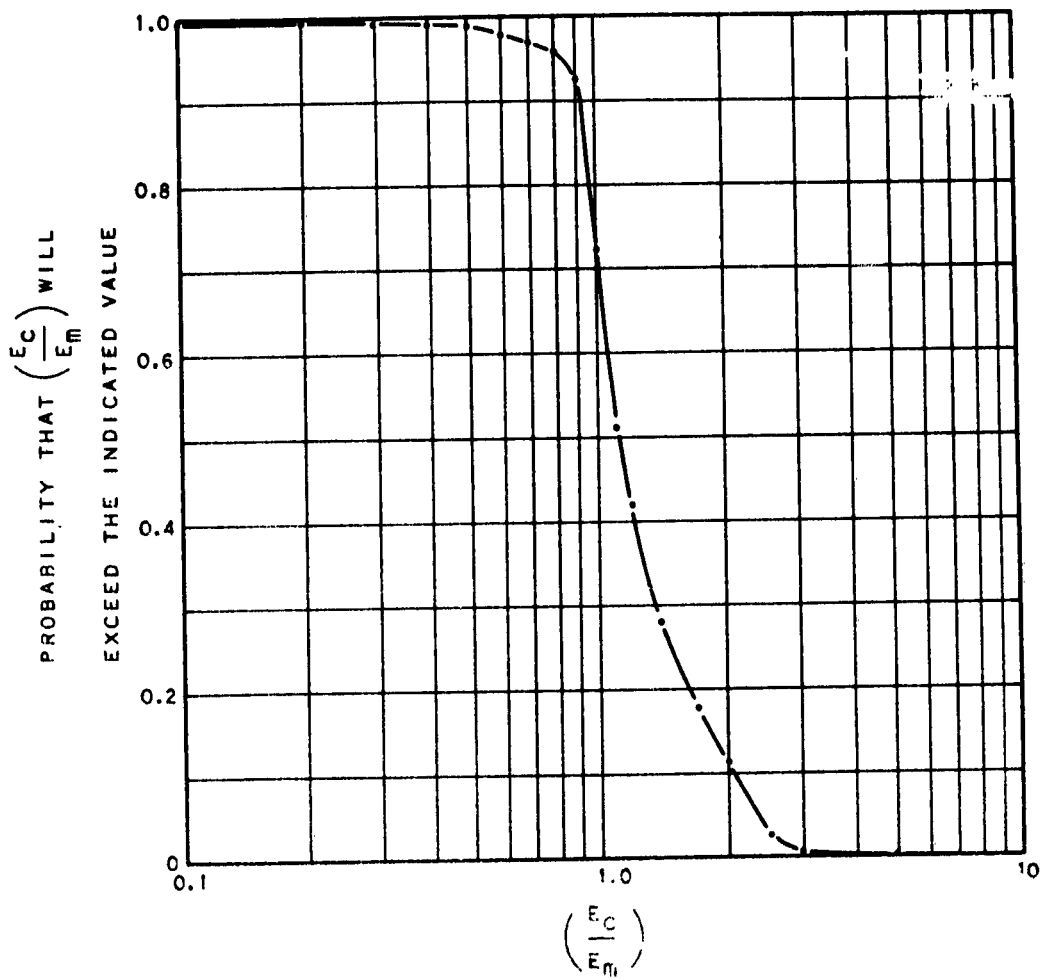


Figure 10. Probability Distribution of  $(E_c/E_m)$  for the Shipboard Area of Figure 9.

not symmetrically disposed about the mean; nevertheless, taking some liberty with statistics, we might say that the standard deviation of the  $X_i$  is approximately 5 db. The results indicate substantial radiation from some structure other than the cage antenna (2-4), either by conduction or mutual impedance, and the presence of considerable standing waves. The two structures immediately suspect are the ship's bridge and the aircraft at the center of the test circle. The results of the next examples tend to show that the aircraft is not the major source of perturbation.

In the next example, Figure 9, the aircraft has been moved to a relatively clear deck area. The transmitting antenna No. 3-5 is a 35-foot vertical whip mounted on a overhanging walkway a few feet below the flight deck level. Again, a total of 156 field strength readings were obtained—144 with the aircraft at the 12 headings and 12 readings with the aircraft removed. The distribution of field strength ratios (computed-to-measured) is given in Figure 10.

In Figure 10, the mean ratio is 1.1. The ratios expressed in decibels ( $X_i$ ) have very nearly a normal distribution with a standard deviation,  $\sigma$ , less than 1.4 db. This is not a large deviation considering the presence of the aircraft, and definitely suggests the feasibility of computing field strengths for certain areas of the ship.

A final example of field strength distributions about the unperturbed field includes measurements made in the areas shown in Figures 11 and 12. Measurements were made at most of the points indicated in Figure 12, once with the aircraft at Point P-3A, again with the aircraft at Point P-3B, and a third time with the aircraft at Point P-3C. Finally, measurements were made with the aircraft removed entirely.

Measurements made in the area of Figure 11 were used as follows: All of the measurements<sup>18</sup> obtained in the areas of Figures 6, 9, 11, and 12 were considered collectively. Figure 13 shows the

---

18. Some of the readings made in the area of Figure 12 (usually several in succession) were in error by an apparent 20 db attenuation step. These were corrected and used only if the error could positively be identified by subsequent measurements, at some point, under nearly identical conditions.

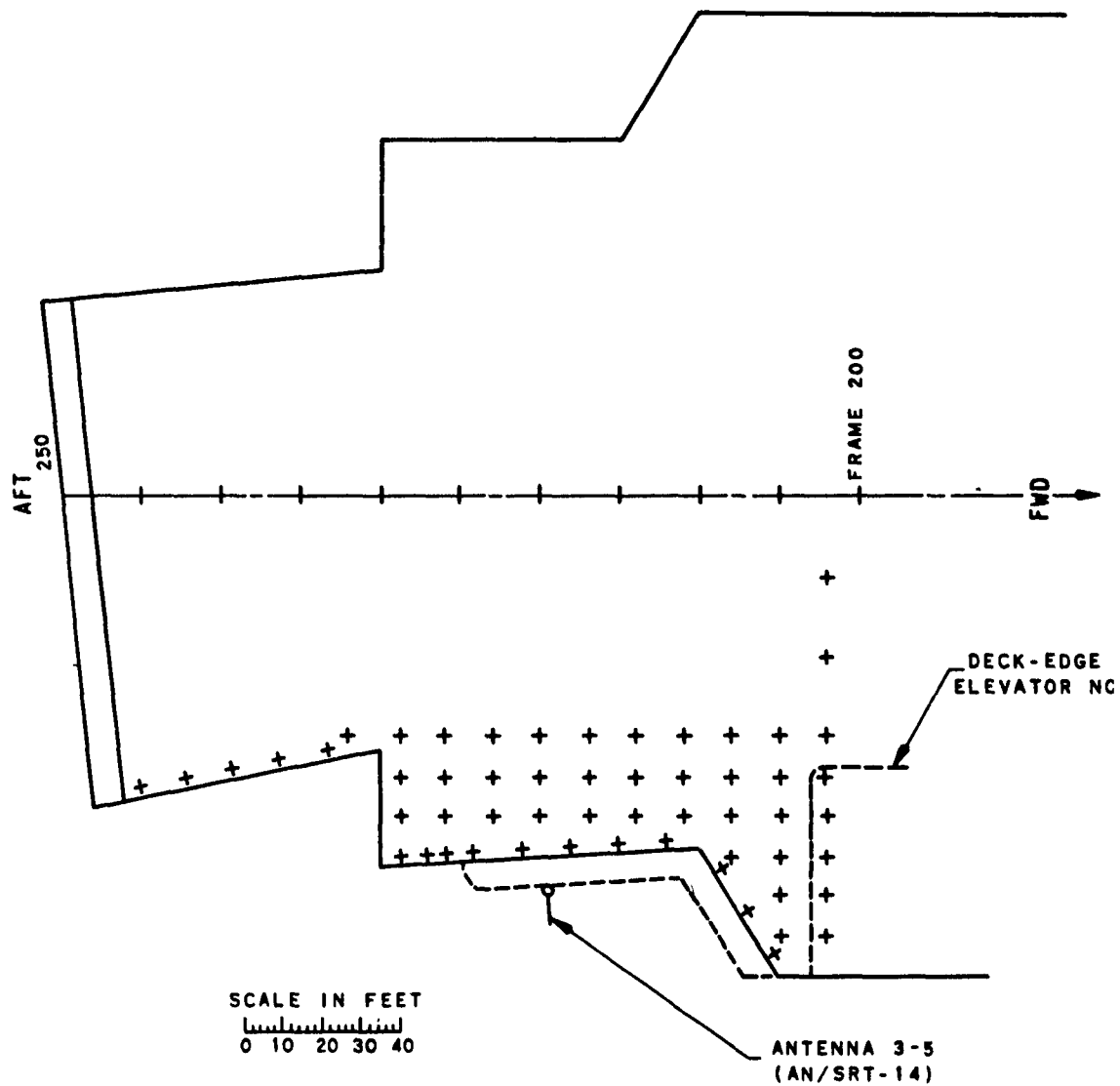


Figure 11. Plan View Showing Test Points for Field Strength Measurements at 9.215 Mc from Antenna 3-5. USS Constellation (CVA-64).

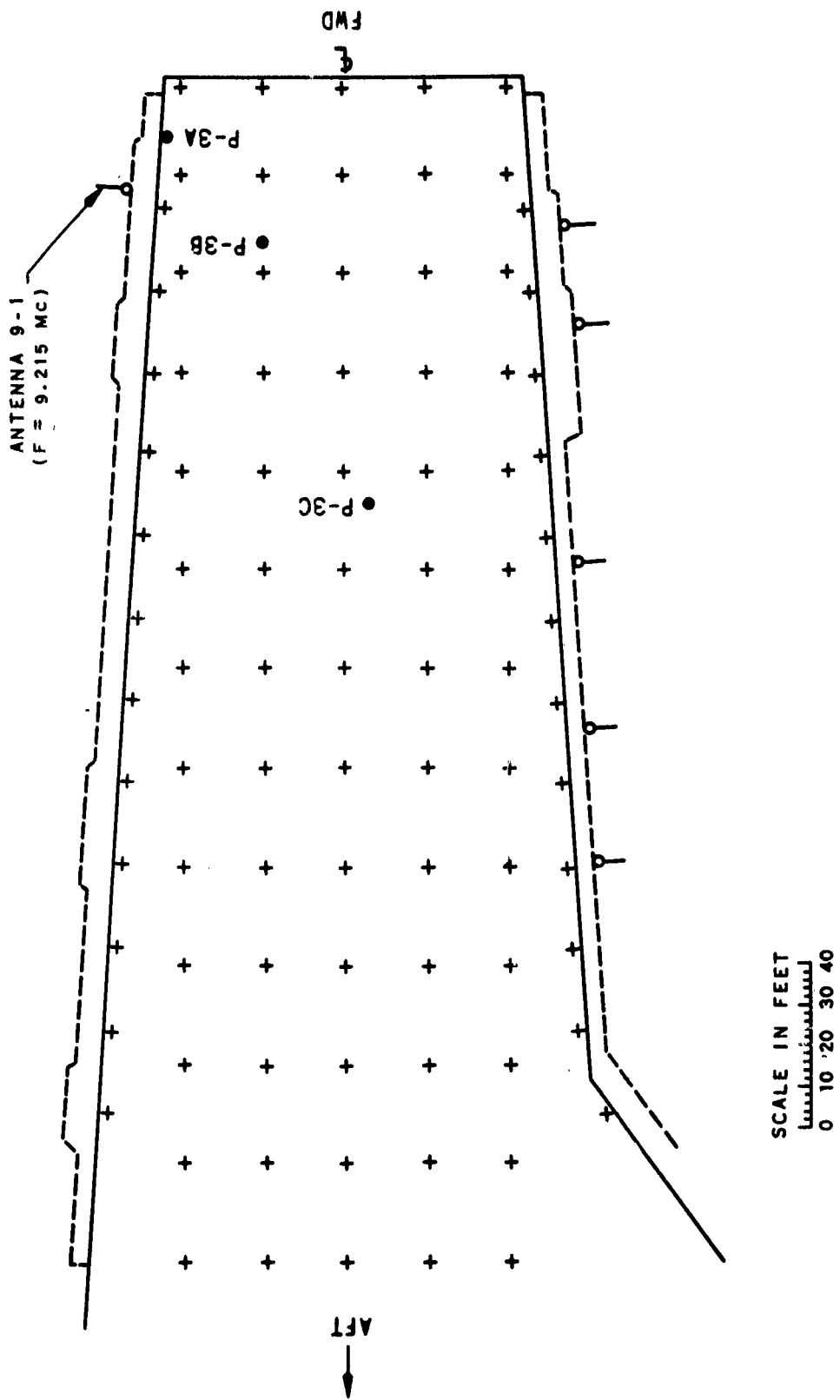


Figure 12. Plan View Showing Test Points for Field Strength Measurements at 9.215 Mc from Antenna 9-1. USS Constellation (CVA-64).

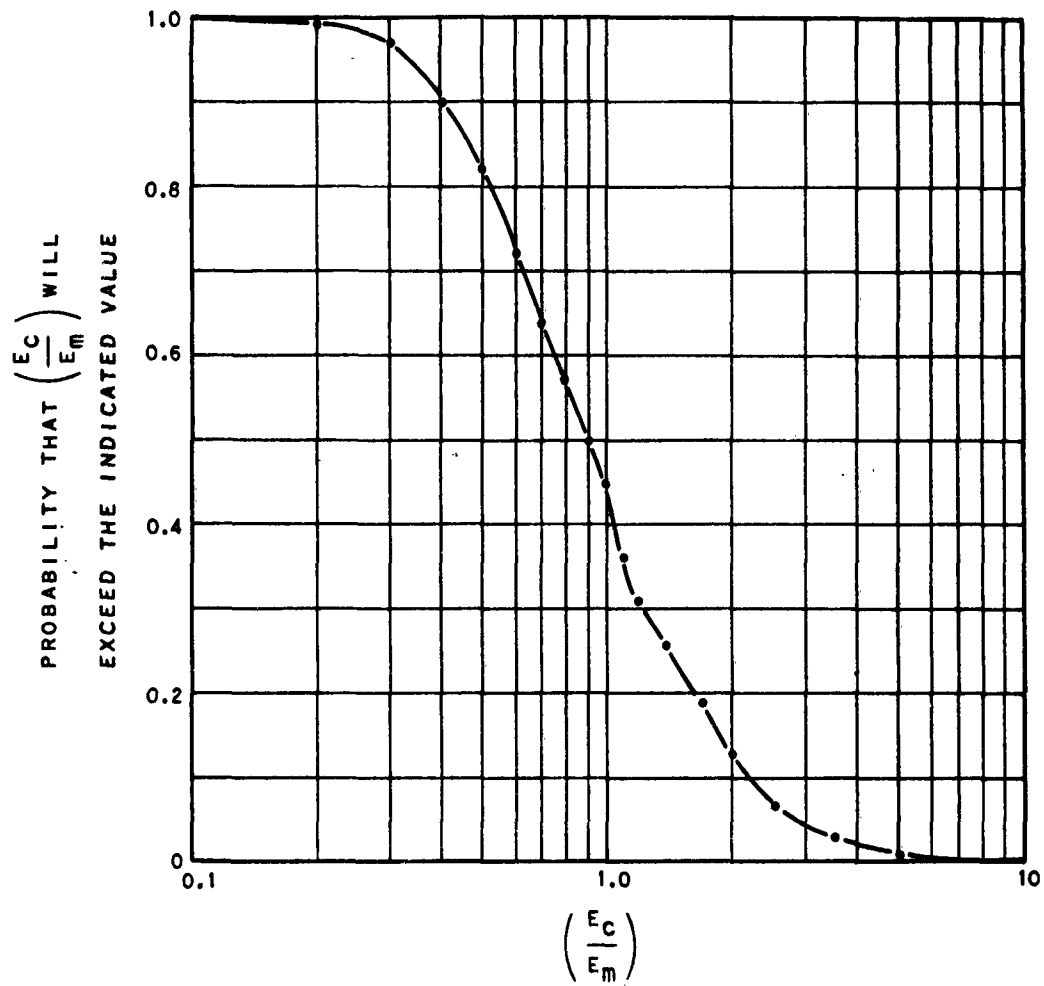


Figure 13. Probability Distribution of  $(E_c/E_m)$  for the Shipboard Areas of Figure 6,9,11 and 12.

probability distribution of the ratios of the computed and measured field strengths (a total of 577 ratios). The mean ratio is 0.9 (see Figure 13). The ratios expressed in decibels ( $X_i$ ) have a very nearly normal distribution with a standard deviation of 4.5 db.

The above procedure establishes a free-space field as a reference, and then accounts for spatial perturbations of the actual field on a statistical basis. It appears that the unobstructed free-space field is a logical reference for the more-or-less open space of an aircraft carrier flight deck. Another reference, such as the diffracted field, might be more logical if the transmitting antenna and receiving area were separated by some large obstacle.

## REFERENCES

1. Electromagnetic Coupling to Ordnance Systems, Jansky & Bailey Division of Atlantic Research Corp., Final Report, Contract N178-7604; August 25, 1961.
2. Handbook of Electroexplosive Devices, Department of Defense, Military Standardization Handbook, MIL-HDBK-219(WEPS); 1 March 1963. (To be printed).
3. Supplement to Project Hero, A Catalog of Equipment Producing and Propagating Electromagnetic Energy, Jansky & Bailey Division of Atlantic Research Corp., Vols. 1 and 2 (Unclassified) and Vol. 3 (Secret); January 1960.
4. Jansky & Bailey Division of Atlantic Research Corp., Internal correspondence with U.S. Naval Weapons Laboratory, Dahlgren, Va.; May 1962.
5. Test Equipment for and Evaluation of Electromagnetic Energy, Denver Research Institute, Vol. 1; November 30, 1960.
6. Research and Development Leading to Perfection of Instrumentation of Electroexplosive Devices, Denver Research Institute, Vol. II; March 31, 1962.
7. Test Equipment for and Evaluation of Electromagnetic Energy, Denver Research Institute, Vol. II; November 30, 1960.
8. Quantum Detector for Measurement of EED Bridge Wire Temperature Rise, Measurement Systems, Inc., Monthly Progress Report No. 1; August 1, 1961.
9. Pneumatic Energy Detector with Remote Optics (PEDRO), Randolph-Macon College, Department of Physics, Quarterly Progress Report No. 1, Report No. 5; October 15, 1961.
10. Field Strength and Fuel Hazard Tests Aboard the USS Constellation (CVA-64), Jansky & Bailey Division of Atlantic Research Corp., Contract No. N0bsr 85503, Task III-3; April 1962.